

Points2Sound: From mono to binaural audio using 3D point cloud scenes

Francesc Lluís

Vasileios Chatzioannou

Alex Hofmann

Department of Music Acoustics (IWK)
 University of Music and Performing Arts Vienna, Austria

lluis-salvado@mdw.ac.at

Abstract

Binaural sound that matches the visual counterpart is crucial to bring meaningful and immersive experiences to people in augmented reality (AR) and virtual reality (VR) applications. Recent works have shown the possibility to generate binaural audio from mono using 2D visual information as guidance. Using 3D visual information may allow for a more accurate representation of a virtual audio scene for VR/AR applications. This paper proposes Points2Sound, a multi-modal deep learning model which generates a binaural version from mono audio using 3D point cloud scenes. Specifically, Points2Sound consist of a vision network which extracts visual features from the point cloud scene to condition an audio network, which operates in the waveform domain, to synthesize the binaural version. Both quantitative and perceptual evaluations indicate that our proposed model is preferred over a reference case, based on a recent 2D mono-to-binaural model.

1. Introduction

We perceive the world through multiple senses that jointly collaborate to understand the environment. Especially for spatial cognition, auditory stimuli, besides visual stimuli, are of paramount importance. For instance, being capable to hear instantly from all angles helps our orientation in space and influences our visual attention. Auditory stimuli are received by both ears and our brain locates sound sources in space by comparing the sound between them. This is known as binaural hearing and it relies mainly on two acoustic cues: Interaural Time Difference (ITD) and Interaural Level Difference (ILD). ITD is the difference in arrival time of a sound between the ears and ILD is the difference in sound intensity. In the median plane, i.e. the vertical plane between the ears, our ITD and ILD are small and we locate sources relying on spectral cues. All these acoustic cues are described by the so called head-related transfer

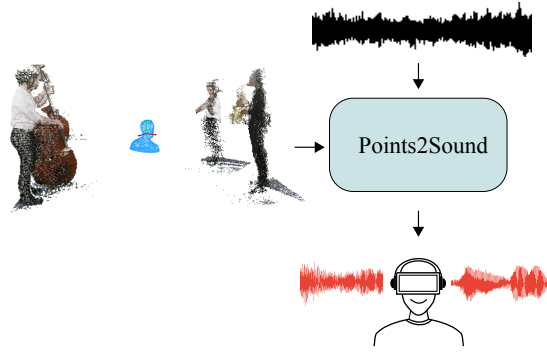


Figure 1. Points2Sound is a deep-learning model capable of generating a binaural version from mono audio that matches a 3D point cloud scene.

function (HRTF), which encodes the sound distortion caused by geometries of the head and the torso [29].

Virtual reality (VR) and augmented reality (AR) systems simulate these binaural acoustic cues in order to match the visual counterpart and achieve users' immersion in the virtual environment. During the interaction with the environment, VR/AR systems manipulate ITD and ILD values for each sound source to infer proper acoustic stimuli according to the user's location and head position [35].

Aiming to enhance immersion in audio-visual experiences, significant progress has been made recently in audio binauralization using visual information. Current methods take into account the limitations of portable devices such as phones when recording audio. Such devices tend to record mono audio which collapses the sound to the same spatial point. For that reason, various methods have been proposed to infer binaural audio from mono recordings using the corresponding 2D video [43, 39, 7, 19].

The incorporation of LiDAR and rgb-depth cameras in portable devices allows to easily capture 3D visual information of the environment and get a more accurate repre-

sentation of the visual scene. This stimulates the creation of algorithms that can guide the binauralization using 3D information and opens new possibilities for VR/AR applications. For instance, considering a captured rgb-depth environment and its corresponding mono audio, one could use an automatic binauralization algorithm to let the users navigate through the virtual environment while inferring proper acoustic stimuli depending on their location and head position.

As a step towards this goal, we introduce Points2Sound, a multimodal neural network capable of synthesizing the binaural version of a mono audio using the 3D point cloud scene of the sound sources in space (see Fig. 1). To our knowledge, we are the first to use point cloud scenes for binaural generation. In addition, as opposed to previous binauralization methods, Points2Sound operates in the waveform domain, which allows to train the multimodal model in a strictly end-to-end fashion. Lastly, quantitative and perceptual evaluations show that Points2Sound significantly outperforms Mono2Binaural, a recent 2D binaural method that we adapt for 3D visual information.

2. Related Work

We provide a brief overview of related works in the field of audio(-visual) source separation and audio-visual spatial audio generation.

Audio(-visual) Source Separation. Source separation has been traditionally approached using only audio signals [1, 10, 34] with methods such as independent component analysis [12], sparse coding [23] or non-negative matrix factorization [16]. Recently, audio source separation has experienced significant progress due to the application of learning methods [40, 20, 28, 31]. Current trends include performing source separation in the waveform domain [30, 18, 3] or preserving binaural cues during the separation process [9, 32]. In addition, deep learning methods have facilitated the inclusion of visual information to guide the audio separation [4, 25]. In the case of music source separation using visual information, learning methods mainly use appearance cues from the 2D visual representations [42, 6], but have been enhanced also with motion information [41, 5]. Lately, 3D visual information such as point clouds have been used also to condition the audio separation [17]. Interestingly, audio-visual source separation models intrinsically learn to map audio to their corresponding position in the visual representation. This has encouraged the use of visual information for spatial audio generation [43].

Audio-visual Spatial Audio Generation. Recently, audio-visual learning for spatial audio generation has

gained interest. Several methods have been proposed to infer spatial acoustic cues to mono audio leveraging visual information. Morgado et al. [22] proposed a learning method to generate the spatial version of mono audio guided by 360°videos. Their approach is to predict the spatial audio in ambisonics format which can be later decoded as binaural audio for reproduction through headphones. Gao et al. [7] show that directly predicting the binaural audio creates better 3D sound sensations. They propose a U-Net-like framework for mono-to-binaural conversion using normal field of view videos. Since then, binauralization models using 2D visual information have been enhanced using different approaches such as using an auxiliary classifier [19] or integrating the source separation task in the overall binaural generation framework [43]. In addition, it has been shown that features from pretrained models on audio-visual spatial alignment tasks are beneficial for audio binauralization [39]. Unlike previous methods, our work tackles visually-informed spatial audio generation directly in the waveform domain. In addition, we use 3D visual information which may allow for a more accurate representation of the entire virtual scene and thereby has potential applicability in VR/AR applications.

3. Approach

We propose Points2Sound, a deep learning algorithm capable of generating a binaural version from a mono audio using the 3D point cloud scene of the sound sources in the space. The code of the proposed algorithm is publicly available¹.

3.1. Problem Formulation

Consider an audio mono signal $s_m \in \mathbb{R}^{1 \times T}$ of length T generated by N sources s_i , with

$$s_m(t) = \sum_{i=1}^N s_i(t) \quad (1)$$

along with the 3D scene of the sound sources in the 3D space represented by a point cloud $\mathcal{V} = \{\mathcal{V}_i\}_{i=1}^P$, and the corresponding binaural signal $s_b \in \mathbb{R}^{2 \times T}$. We aim at finding a model f with the structure of a neural network such that $s_b(t) = f(s_m(t), \mathcal{V})$. The binaural version $s_b(t)$ generated by N sources s_i is defined as:

$$s_b^{L,R}(t) = \sum_{i=1}^N s_i(t) \circledast \text{HRTF}(\varphi_i, \theta_i)|_{\text{left,right}} \quad (2)$$

where $\text{HRTF}(\varphi_i, \theta_i)|_{\text{left,right}}$ is the head-related transfer function of the sound incidence at the specified i -source

¹<https://github.com/francescluis/points2sound>

orientation (φ_i, θ_i) for both left (L) and right (R) ears. Throughout this work, orientation is defined based on a head-related coordinate system, i.e. the center of coordinates is considered the head of the listener.

3.2. Points2Sound Model Architecture

We propose a multi-modal neural network architecture capable of synthesizing binaural audio in an end-to-end fashion: the architecture takes as inputs the raw mono waveform along with the 3D point cloud scene and outputs the corresponding binaural waveform. The architecture comprises a vision network and an audio network. Broadly, the vision network extracts a visual feature from the 3D point cloud scene that serves to condition the audio network for binaural synthesis. Figure 2 shows a schematic diagram of the proposed model.

Sparse Tensor and 3D Sparse Convolution. As a first step, the point cloud scene \mathcal{V} , with its corresponding coordinates \mathcal{C} and associated features \mathcal{F} , is represented by a third order tensor $\mathbf{T} \in \mathbb{R}^{N_1 \times N_2 \times N_3}$. To this end, a voxel size v_s is used to define point cloud coordinates in the integer grid of the tensor i.e. $\mathcal{C}' = \lfloor \frac{\mathcal{C}}{v_s} \rfloor$. Due to the amount of empty space a point cloud contains, the resultant sparse tensor is made of only a few non-zero elements.

$$\mathbf{T}[\mathbf{c}'_i] = \begin{cases} \mathbf{f}_i & \text{if } \mathbf{c}'_i \in \mathcal{C}' \\ 0 & \text{otherwise,} \end{cases} \quad (3)$$

where $\mathcal{C}' = \text{supp}(\mathbf{T})$ is the set of non-zero discretized coordinates and \mathbf{f}_i is the feature associated to \mathcal{V}_i . Then, considering predefined input coordinates \mathcal{C}'_{in} and output coordinates $\mathcal{C}'_{\text{out}}$, convolution on a 3D sparse tensor can be defined as follows:

$$\mathbf{T}'[x, y, z] = \sum_{i, j, k \in \mathcal{N}(x, y, z)} \mathbf{W}[i, j, k] \mathbf{T}[x + i, y + j, z + k] \quad (4)$$

for $(x, y, z) \in \mathcal{C}'_{\text{out}}$. Where $\mathcal{N}(x, y, z) = \{(i, j, k) | |i| \leq L, |j| \leq L, |k| \leq L, (i + x, j + y, k + z) \in \mathcal{C}'_{\text{in}}\}$. \mathbf{W} are the weights of the 3D convolutional kernel and $2L + 1$ is the convolution kernel size.

Vision Network. The vision network consists of a Resnet18 [11] architecture with 3D sparse convolutions [2] that extracts a visual feature from the 3D point cloud scene. Resnet18 with 3D sparse convolutions has been successfully used in several tasks such as 3D semantic segmentation [2], 3D single-shot object detection [8], and audio source separation conditioned on 3D point clouds [17]. Thus, we consider sparse Resnet18 suitable for our scenario, where extracting information about the location of the sources while recognizing the type of source is critical for reliable binaural synthesis. Sparse Resnet18 learns at

different scales by halving the feature space after two residual blocks and doubling the receptive field by using a stride of 2. Through the network, ReLU is used as activation function and batch normalization is applied after sparse convolutions. At the top of Resnet18 4th block, we add a 3x3x3 sparse convolution with $K = 16$ output channels and apply a max-pooling operation to adequate the dimensions of the extracted visual feature \mathbf{h} .

Audio Network. We adopt the Demucs architecture [3] to synthesise binaural versions \hat{s}_b from mono audio signals s_m given the 3D scene of the sound sources \mathcal{V} . Although Demucs was originally designed for source separation, we find it appropriate for binaural synthesis because the model needs to intrinsically learn to separate the sound of the sources in the mono mixture for further rendering (see Eq. 2). In addition, it operates at 44.1 kHz which helps to synthesize binaural nuances in the higher frequency range. Demucs works in the waveform domain and has a U-Net-like structure [27] (see Fig. 2). The encoder-decoder structure learns multi-resolution features from the raw waveform while skip connections allow low-level information to be propagated through the network, such as the phase of the input signal. In this work, we keep the Demucs parameters from its original configuration and only adapt the input and output channels to match our mono and binaural signals.

Conditioning. We use a global conditioning approach on the audio network to guide the binaural synthesis according to the 3D scene. Global conditioning has been successfully used in Demucs for separation purposes using one-hot vectors [13]. In a similar way, we use the the extracted visual feature \mathbf{h} from the vision network and insert it in each encoder and decoder block of the audio network. Specifically, the visual feature is inserted after being multiplied by a learnable linear projection $\mathbf{V}_{\cdot, k, \cdot}$. As in [13], Demucs encoder and decoder takes the following expression:

$$\begin{aligned} \text{Encoder}_{k+1} = & \text{GLU}(\mathbf{W}_{\text{encoder}, k, 2} * \text{ReLU}(\mathbf{W}_{\text{encoder}, k, 1} * \\ & \text{Encoder}_k + \mathbf{V}_{\text{encoder}, k, 1} \mathbf{h}) + \mathbf{V}_{\text{encoder}, k, 2} \mathbf{h}), \end{aligned} \quad (5)$$

$$\begin{aligned} \text{Decoder}_{k-1} = & \text{ReLU}(\mathbf{W}_{\text{decoder}, k, 2} *^{\top} \text{GLU}(\mathbf{W}_{\text{decoder}, k, 1} * \\ & (\text{Encoder}_k + \text{Decoder}_k) + \mathbf{V}_{\text{decoder}, k, 1} \mathbf{h}) \\ & + \mathbf{V}_{\text{decoder}, k, 2} \mathbf{h}). \end{aligned} \quad (6)$$

where Encoder_{k+1} and Decoder_{k-1} are the outputs from the k level encoder and decoder blocks respectively. $\mathbf{W}_{\cdot, k, \cdot}$ are the 1-D kernel weights at the k block and ReLU/GLU are the corresponding activation functions.

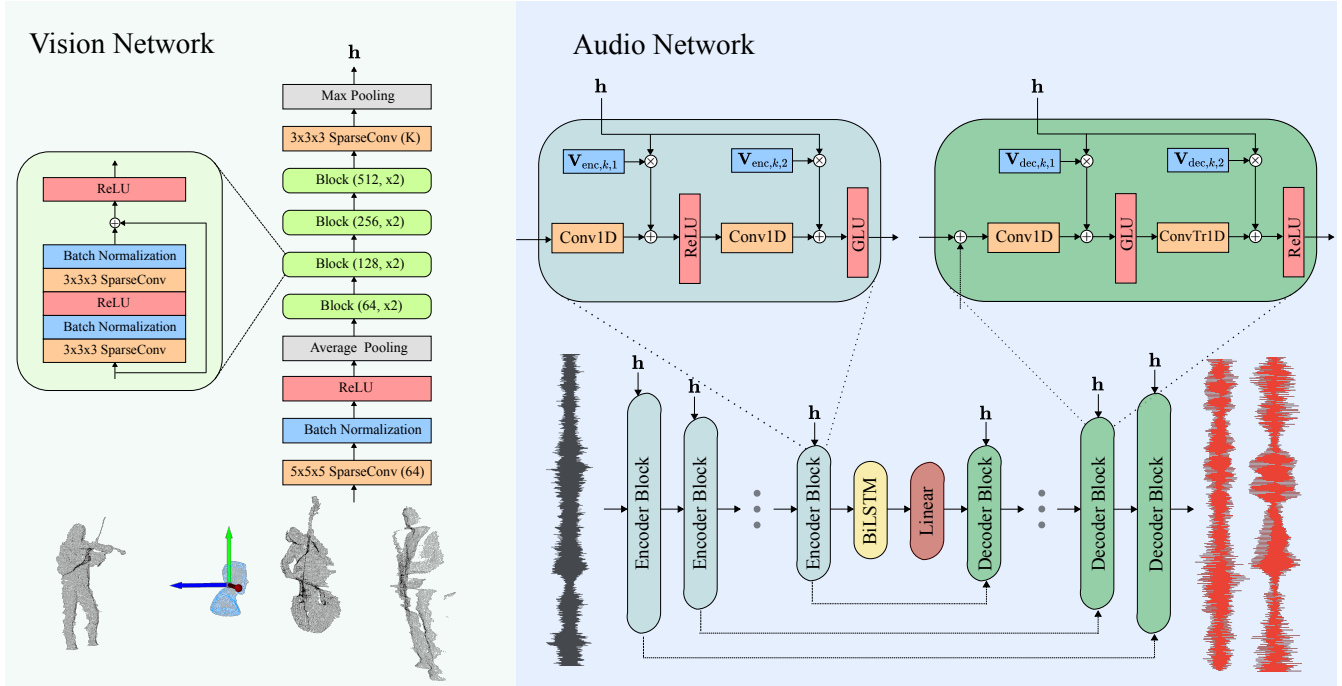


Figure 2. Overview diagram of Points2Sound. It consists of a sparse Resnet18 network for visual analysis and a Demucs network for binaural audio synthesis. The vision network extracts a visual feature h from the 3D point cloud. Then, this visual feature serves to condition the audio network to generate a binaural version from the mono audio that matches the visual counterpart. Both networks are jointly trained optimizing the L1 loss between the predicted and the ground truth binaural waveforms.

Learning Objective. During the training of Points2Sound, the parameters of the model are optimized to reduce the L1 loss function between the estimated binaural \hat{s}_b and the ground truth binaural s_b .

3.3. Data

We compile a dataset by taking material from several sources [33, 17, 14, 21, 42] in the form of 3D point clouds and audio recordings of musicians playing five different instruments: cello, double bass, guitar, saxophone, and violin. This data will serve later to generate 3D audio-visual scenes for self-supervised learning.

Point Clouds. We compile musician point clouds from *3D video source separation* [17], *small ensemble 3D-video database* [33], and *Panoptic Studio* [14]. In *3D video source separation*, point cloud recordings are captured using a single Azure Kinect DK. Recordings span 1 hour of duration with an average of 12 different performers for each of the instruments. In *small ensemble 3D-video database*, recordings are carried out using three RGB-Depth Kinect v2 sensors. The average video recording is 5 minutes per instrument with a single performer. In *Panoptic Studio*, recordings are carried out using ten Kinect sensors. In this case, only cello and guitar recordings are available with an average of 2 minutes per instrument with a single performer.

Once all point cloud recordings are collected, we split 75% of the data for training, 15% for validation, and the remaining 10% for testing. Data split is made ensuring that there is no overlap in identities between sets.

Audio. We collect 30 hours of mono audio recordings at 44.1 kHz from *Solos* [21] and *Music* [42]. Both datasets gather music from YouTube which ensures a variety of acoustic conditions. In total, we gather 72 recordings per instrument with an average of 5 minutes per recording. We split 75% of the recordings for training, 15% for validation, and the remaining 10% for testing.

For further binaural auditory scene generation, we also create multiple binaural versions of each recording using the *Two!Ears* Binaural Simulator [37]. Specifically, for each audio recording we simulate the binaural version at a discrete set of angular positions in the horizontal plane with no elevation, i.e. $(\varphi_k, \theta) := (\frac{k\pi}{4}, 0)$ for $k = 0, \dots, 7$. For binaural auditory modelling, we use the HRTFs at 1m of distance between source and receiver measured with a KEMAR dummy head at the anechoic chamber of the TU Berlin [36].

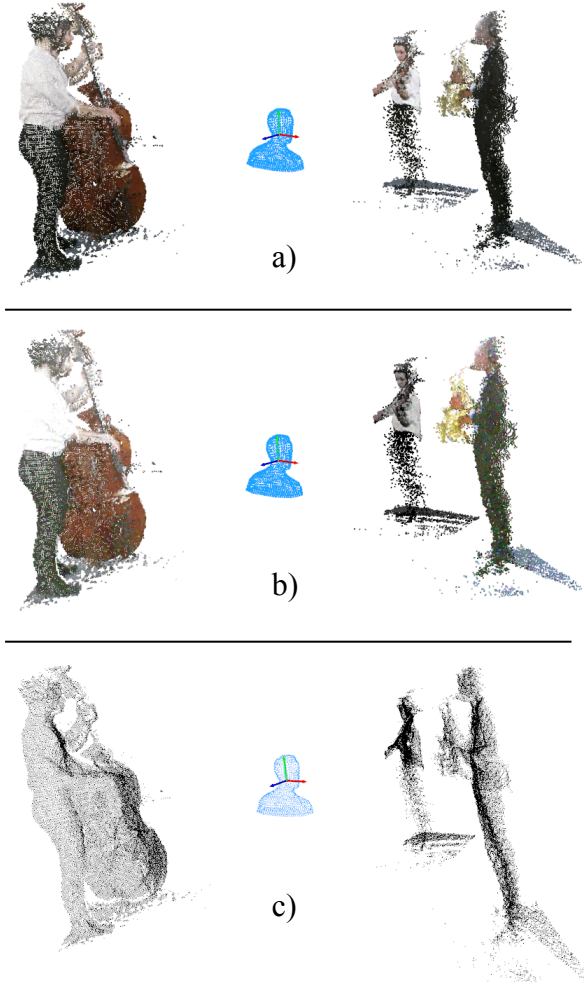


Figure 3. Illustration of the augmentation operations applied to a 3D point cloud scene. a) Original. b) Color augmentations. c) Coordinate augmentations.

3.4. Audio-visual 3D Scene Generation for Self-supervised Learning

We synthetically create mono mixtures, 3D scenes, and the corresponding binaural version to train the model in a self-supervised fashion.

For each instance, we randomly select N sources and N angular positions with N chosen uniformly between 1 and 3. Then, mono mixtures are created by selecting individual mono samples of 3 s length from these sources and mixing them together following Eq. 1. The binaural version of the mono mixture, which serves as supervision, is created following Eq. 2. First, we select the binaural version for each sound source in the mix based on its angular position, and then we sum all selected binaural signals to create the binaural mixture.

For the 3D scene, we first select individual-musician’s

point clouds corresponding to these sources. Then, musician point clouds are located at their corresponding angular position in a random distance ranging from 1 to 3 meters from the listeners head in the 3D space. Finally, all N musician point clouds are merged to create a single 3D point cloud scene. Note that we generate binaural versions using HRTFs computed at 1 meter distance from the listeners head but locate the sources in a distance ranging from 1 to 3 meters. This assumption is based on the fact that distance has almost no influence on the shape of HRTFs, for source-receiver distances greater than 1m [24].

During the training of the model, each individual musician point cloud is independently augmented in both coordinates and color. We randomly shear and translate the coordinates of each musician in the scene. Shearing is applied along all axes and the shear elements are sampled from a Normal distribution $\mathcal{N}(0, 0.1^2)$. Translation is applied along the stature direction and the translation offset is sampled from $\mathcal{N}(0, 0.2^2)$.

Regarding color, we distort the brightness and intensity of each sound source in the scene. Specifically, we apply color distortion to each point via adding Gaussian noise sampled from $\mathcal{N}(0, 0.05^2)$ on each rgb color channel. We also alter color value and color saturation with random amounts uniformly sampled ranging from -0.2 to 0.2 and -0.15 to 0.15 respectively. Figure 3 illustrates the different augmentation operations applied. After augmentation, each scene is represented as a sparse tensor by discretizing the point cloud coordinates using a voxel size of 0.02.

4. Experimental Results

4.1. Implementation Details

Initially, we pretrain the vision network to facilitate the future learning process. Pretraining is done on the 3D object classification task modelnet40 [38]. Since modelnet40 consists of 3D CAD models, we sample point clouds from the mesh surface of the objects shapes. For the pretraining, we also discretize the coordinates setting the voxel size to 0.02. Then, Points2Sound vision and audio networks are jointly trained for 120k iterations using the Adam [15] optimizer. We use a batch size of 40 samples and we set the learning rate to 1×10^{-4} . We select the weights with less validation loss after the training process. Training and testing are conducted on a single Titan RTX GPU. We use the Minkowski Engine [2] for the sparse tensor operations and PyTorch [26] for the other operations required.

4.2. Evaluation Metrics

We measure the quality of the predicted binaural audio assessing the Envelope Distance and the short-time Fourier transform (STFT) Distance. Envelope Distance (d_{ENV}) and STFT Distance (d_{STFT}) between a binaural signal s_b and

Visual features		d _{ENV}			d _{STFT}			d _{ENV}	d _{STFT}
		1	2	3	1	2	3		
Mono-Mono	-	0.107	0.085	0.077	2.996	1.455	1.045	0.090	1.832
Rotated-Visual	depth	0.127	0.092	0.078	3.615	1.561	1.023	0.099	2.066
	rgb-depth	0.127	0.093	0.081	3.592	1.648	1.107	0.100	2.116
Mono2Binaural[7]	depth	0.101	0.080	0.072	1.146	0.666	0.531	0.085	0.781
	rgb-depth	0.102	0.081	0.073	1.181	0.710	0.555	0.085	0.815
Points2Sound (ours)	depth	0.026	0.041	0.046	0.086	0.211	0.242	0.038	0.180
	rgb-depth	0.026	0.039	0.042	0.113	0.185	0.209	0.036	0.169

Table 1. Quantitative results of baselines and Points2Sound. For each method, we report the performance depending to the number of sources ($N = 1, 2, 3$), the type of 3D scenes (depth or rgb-depth), and its average.

its estimate \hat{s}_b are defined as:

$$\begin{aligned} d_{ENV} = & \|E[s_b^L(t)] - E[\hat{s}_b^L(t)]\|_2 + \\ & \|E[s_b^R(t)] - E[\hat{s}_b^R(t)]\|_2 \end{aligned} \quad (7)$$

$$\begin{aligned} d_{STFT} = & \|\text{STFT}(s_b^L(t)) - \text{STFT}(\hat{s}_b^L(t))\|_2 + \\ & \|\text{STFT}(s_b^R(t)) - \text{STFT}(\hat{s}_b^R(t))\|_2 \end{aligned} \quad (8)$$

where $\|\cdot\|_2$ is the L2 norm, $E[s(t)]$ corresponds to the envelope of the signal $s(t)$, and $\text{STFT}(\cdot)$ is the short-time Fourier transform. The envelope is computed as the absolute value of the analytical signal and the STFT is computed using a Hann window of 23 ms and hop length of 10 ms.

4.3. Baselines

We use 3 baselines to assess the quality of the predicted binaural versions:

Mono2Binaural[7]. For comparison, we use the spectrogram-based *Mono2Binaural* model from Gao et al. [7]. *Mono2Binaural* was designed to generate a binaural version from mono audio at 16 kHz using 2D visual information as guidance. For the purposes of this work, we adapt it for audio recordings sampled at 44.1 kHz and 3D visual information as guidance. The original *mono2binaural* extracts visual features using a Resnet18 with dense convolutions while audio features and audio-visual analysis is performed using a U-Net. In this work, we use the same sparse Resnet18 from Points2Sound to extract the visual feature from the 3D scene. In addition, in order to resemble its original model, the last Resnet18 3x3x3 sparse convolution is implemented with $K = 512$ channels. Then, as in *mono2binaural*, the visual feature vector is replicated to match the spatial feature dimensions of the U-Net bottleneck and concatenated along the channel dimension. During training, we select 0.63 s clips of audio and compute the STFT using a Hann window of 23 ms and hop length of 10 ms. The learning objective is to predict the complex-valued spectrogram of the difference of the two binaural channels. We use Adam optimizer and minimize

the MSE loss. During testing, *mono2binaural* uses a sliding window with a hop size of 0.05 s to binauralize the 10 s audio clips.

Rotated-Visual. Rotated-Visual baseline assesses the performance of Points2Sound when wrong visual information is provided. To this end, during testing we rotate the 3D scene by $\pi/2$ in the horizontal plane of the listener’s head.

Mono-Mono. Mono-Mono baseline simply copies the mono input audio to both binaural predicted channels.

4.4. Results

4.4.1 Quantitative

We are interested in evaluating the quality of the predicted binaural audio depending on the number of sound sources present in the 3D scene. To this end, for evaluation we use 500 audio-visual 3D scenes with $N = 1, 2, 3$ sound sources. Audio-visual 3D scenes are generated using the test data set and following the procedure explained in section 3.4. Note that during evaluation, augmentation operations are not applied and 10 second audio clips are selected. In addition, the predicted binaural audio is evaluated considering two types of 3D scenes: when 3D scenes consist of depth-only data and when 3D scenes consist of rgb-depth data. In the cases where depth-only information is available, we use the non-discretized coordinates as the feature vectors associated to each point. When rgb-depth information is available, we use the rgb values as the feature vectors associated to each point.

Results in Table 4 show that our method Points2Sound outperforms the baselines with a considerable margin. Regarding 3D visual conditioning, Points2Sound results are slightly better for multiple sources when using rgb-depth information. This suggest that rgb information helps the model to recognize and locate multiple sources in the 3D space. Informal listening corroborates that rgb-depth conditioning provides more stable auditory images of the sound sources for the whole 10 second clips. Worst results are obtained with the rotated-visual baseline. This indicates

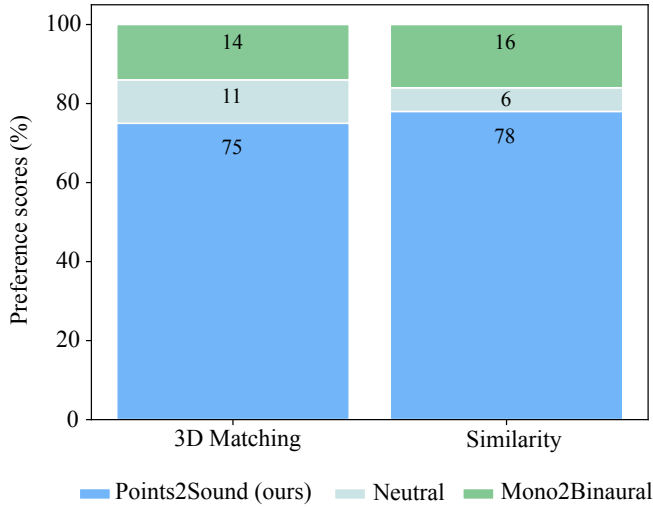


Figure 4. Subjective preference scores (%) of predicted binaural samples between Points2Sound and Mono2Binaural.

that Points2Sound strongly relies in the 3D scene to synthesize binaural audio and incorrect predictions are expected when using wrong visual information. Mono2Binaural performs better than the Mono-Mono baseline especially in the metric it has been optimized during the training, i.e. d_{STFT} . However, Mono2Binaural doesn't benefit from the rgb information of the 3D scene and performance improves as more sources are present in the audio-visual scene. In Mono2Binaural, we found that optimizing the model with regard to the difference between binaural channels leads to conservative predictions. This results in poorer predictions with only one source due to a bigger difference between ground truth binaural channels. In early experiments, we also optimized Points2Sound with regard to the difference between binaural channels and observed the same effect.

4.4.2 Qualitative

We performed blind perceptual tests with 18 participants to get subjective feedback on the effectiveness of Points2Sound. Ten scenes from the test set are selected with their corresponding 10 s audio clips. For each instance, participants listen to the ground truth binaural audio and the predicted binaural audio of Points2Sound and Mono2Binaural. Participants are asked two questions: *i)* *Which of the predicted audio matches better the 3D scene?* and *ii)* *Which of the predicted audio is similar to the ground truth audio?*. Participants can listen to the audio clips multiple times and a *Neutral* option is given in the case there is no preference between the predicted audios.

Results in Figure 4 show that participants consider binaural audio predicted by Points2Sound to match better the 3D scene and be similar to the ground truth audio. However,

although Points2Sound is mostly preferred for both testing conditions, some of the participants noted that it introduces some artifacts in the form of high frequency noise.

5. Conclusion

This work introduced Points2Sound, a multi-modal deep learning model capable of generating a binaural version from mono audio that matches a 3D point cloud scene. As opposed to previous audio-visual binauralization methods, Points2Sound operates in the waveform domain and uses 3D visual information. Quantitative and qualitative results show the effectiveness of our proposed model which enables potential applicability in VR/AR applications. Future work includes adding loudness into the learning process via predicting a reference sound level for each source. This will allow to consider distances between the source and the listener and infer also sound attenuation in 3D dynamic scenes.

6. Acknowledgments

This project has received funding from the European Union's Horizon 2020 research and innovation programme under the Marie Skłodowska-Curie grant agreement No 812719.

7. Author Contributions

FL proposed the idea, wrote the code, ran the experiments and wrote the paper. **VC** and **AH** supervised the research.

References

- [1] J-F Cardoso. Blind signal separation: statistical principles. *Proceedings of the IEEE*, 86(10):2009–2025, 1998.
- [2] Christopher Choy, JunYoung Gwak, and Silvio Savarese. 4d spatio-temporal convnets: Minkowski convolutional neural networks. In *Proceedings of the IEEE Conference on Computer Vision and Pattern Recognition*, pages 3075–3084, 2019.
- [3] Alexandre Défossez, Nicolas Usunier, Léon Bottou, and Francis Bach. Music source separation in the waveform domain. *arXiv preprint arXiv:1911.13254*, 2019.
- [4] Ariel Ephrat, Inbar Mosseri, Oran Lang, Tali Dekel, Kevin Wilson, Avinatan Hassidim, William T Freeman, and Michael Rubinstein. Looking to listen at the cocktail party: A speaker-independent audio-visual model for speech separation. *arXiv preprint arXiv:1804.03619*, 2018.
- [5] Chuang Gan, Deng Huang, Hang Zhao, Joshua B Tenenbaum, and Antonio Torralba. Music gesture for visual sound separation. In *Proceedings of the IEEE/CVF Conference on Computer Vision and Pattern Recognition*, pages 10478–10487, 2020.
- [6] Ruohan Gao, Rogerio Feris, and Kristen Grauman. Learning to separate object sounds by watching unlabeled video. In

Proceedings of the European Conference on Computer Vision (ECCV), pages 35–53, 2018.

[7] Ruohan Gao and Kristen Grauman. 2.5 d visual sound. In *Proceedings of the IEEE/CVF Conference on Computer Vision and Pattern Recognition*, pages 324–333, 2019.

[8] JunYoung Gwak, Christopher Choy, and Silvio Savarese. Generative sparse detection networks for 3d single-shot object detection. *arXiv preprint arXiv:2006.12356*, 2020.

[9] Cong Han, Yi Luo, and Nima Mesgarani. Real-time binaural speech separation with preserved spatial cues. In *ICASSP 2020-2020 IEEE International Conference on Acoustics, Speech and Signal Processing (ICASSP)*, pages 6404–6408. IEEE, 2020.

[10] Simon Haykin and Zhe Chen. The cocktail party problem. *Neural computation*, 17(9):1875–1902, 2005.

[11] Kaiming He, Xiangyu Zhang, Shaoqing Ren, and Jian Sun. Deep residual learning for image recognition. In *Proceedings of the IEEE conference on computer vision and pattern recognition*, pages 770–778, 2016.

[12] Aapo Hyvärinen and Erkki Oja. Independent component analysis: algorithms and applications. *Neural networks*, 13(4-5):411–430, 2000.

[13] Teerapat Jenrungrot, Vivek Jayaram, Steve Seitz, and Ira Kemelmacher-Shlizerman. The cone of silence: Speech separation by localization. In *Advances in Neural Information Processing Systems*, 2020.

[14] Hanbyul Joo, Tomas Simon, Xulong Li, Hao Liu, Lei Tan, Lin Gui, Sean Banerjee, Timothy Godisart, Bart Nabbe, Iain Matthews, et al. Panoptic studio: A massively multiview system for social interaction capture. *IEEE transactions on pattern analysis and machine intelligence*, 41(1):190–204, 2017.

[15] Diederik P Kingma and Jimmy Lei Ba. Adam: A method for stochastic gradient descent. In *ICLR: International Conference on Learning Representations*, pages 1–15, 2015.

[16] D Lee and SH Sebastian. Algorithms for non-negative matrix factorization, advances in neural information processing systems. In *Proceedings of the 2000 Conference*, pages 556–562, 2000.

[17] Francesc Lluís, Vasileios Chatzioannou, and Alex Hofmann. Music source separation conditioned on 3d point clouds. *arXiv preprint arXiv:2102.02028*, 2021.

[18] Francesc Lluís, Jordi Pons, and Xavier Serra. End-to-end music source separation: Is it possible in the waveform domain? In *Interspeech*, 2019.

[19] Yu-Ding Lu, Hsin-Ying Lee, Hung-Yu Tseng, and Ming-Hsuan Yang. Self-supervised audio spatialization with correspondence classifier. In *2019 IEEE International Conference on Image Processing (ICIP)*, pages 3347–3351. IEEE, 2019.

[20] Yi Luo and Nima Mesgarani. Conv-tasnet: Surpassing ideal time–frequency magnitude masking for speech separation. *IEEE/ACM transactions on audio, speech, and language processing*, 27(8):1256–1266, 2019.

[21] Juan F Montesinos, Olga Slizovskaia, and Gloria Haro. Sолос: A dataset for audio-visual music analysis. In *2020 IEEE 22nd International Workshop on Multimedia Signal Processing (MMSP)*, pages 1–6. IEEE, 2020.

[22] Pedro Morgado, Nuno Vasconcelos, Timothy Langlois, and Oliver Wang. Self-supervised generation of spatial audio for 360° video. In *Proceedings of the 32nd International Conference on Neural Information Processing Systems*, pages 360–370, 2018.

[23] Bruno A Olshausen and David J Field. Sparse coding with an overcomplete basis set: A strategy employed by v1? *Vision research*, 37(23):3311–3325, 1997.

[24] Makoto Otani, Tatsuya Hirahara, and Shiro Ise. Numerical study on source-distance dependency of head-related transfer functions. *The Journal of the Acoustical Society of America*, 125(5):3253–3261, 2009.

[25] Andrew Owens and Alexei A Efros. Audio-visual scene analysis with self-supervised multisensory features. In *Proceedings of the European Conference on Computer Vision (ECCV)*, pages 631–648, 2018.

[26] Adam Paszke, Sam Gross, Francisco Massa, Adam Lerer, James Bradbury, Gregory Chanan, Trevor Killeen, Zeming Lin, Natalia Gimelshein, Luca Antiga, et al. Pytorch: An imperative style, high-performance deep learning library. In *Advances in neural information processing systems*, pages 8026–8037, 2019.

[27] Olaf Ronneberger, Philipp Fischer, and Thomas Brox. U-net: Convolutional networks for biomedical image segmentation. In *International Conference on Medical image computing and computer-assisted intervention*, pages 234–241. Springer, 2015.

[28] David Samuel, Aditya Ganeshan, and Jason Naradowsky. Meta-learning extractors for music source separation. In *ICASSP 2020-2020 IEEE International Conference on Acoustics, Speech and Signal Processing (ICASSP)*, pages 816–820. IEEE, 2020.

[29] EAG Shaw. External ear response and sound localization. *Localization of sound: Theory and applications*, pages 30–41, 1982.

[30] Daniel Stoller, Sebastian Ewert, and Simon Dixon. Wave-u-net: A multi-scale neural network for end-to-end audio source separation. *ISMIR*, 2018.

[31] Naoya Takahashi and Yuki Mitsufuji. Densely connected multidilated convolutional networks for dense prediction tasks. *arXiv preprint arXiv:2011.11844*, 2020.

[32] Ke Tan, Buye Xu, Anurag Kumar, Eliya Nachmani, and Yossi Adi. Sagrnn: Self-attentive gated rnn for binaural speaker separation with interaural cue preservation. *IEEE Signal Processing Letters*, 2020.

[33] David Thery and Brian Katz. Anechoic audio and 3d-video content database of small ensemble performances for virtual concerts. In *23rd International Congress on Acoustics*, pages 739–46. German Acoustical Society (DEGA), 2019.

[34] Emmanuel Vincent, Tuomas Virtanen, and Sharon Gannot. *Audio source separation and speech enhancement*. John Wiley & Sons, 2018.

[35] Michael Vorländer. *Auralization*. Springer, 2020.

[36] Hagen Wierstorf, Matthias Geier, and Sascha Spors. A free database of head related impulse response measurements in the horizontal plane with multiple distances. In *Audio Engineering Society Convention 130*. Audio Engineering Society, 2011.

- [37] Fiete Winter, Hagen Wierstorf, Alexander Raake, and Sascha Spors. The two! ears database. In *Audio Engineering Society Convention 142*. Audio Engineering Society, 2017.
- [38] Zhirong Wu, Shuran Song, Aditya Khosla, Fisher Yu, Lin-guang Zhang, Xiaoou Tang, and Jianxiong Xiao. 3d shapenets: A deep representation for volumetric shapes. In *Proceedings of the IEEE conference on computer vision and pattern recognition*, pages 1912–1920, 2015.
- [39] Karren Yang, Bryan Russell, and Justin Salamon. Telling left from right: Learning spatial correspondence of sight and sound. In *Proceedings of the IEEE/CVF Conference on Computer Vision and Pattern Recognition*, pages 9932–9941, 2020.
- [40] Neil Zeghidour and David Grangier. Wavesplit: End-to-end speech separation by speaker clustering. *arXiv preprint arXiv:2002.08933*, 2020.
- [41] Hang Zhao, Chuang Gan, Wei-Chiu Ma, and Antonio Torralba. The sound of motions. In *Proceedings of the IEEE International Conference on Computer Vision*, pages 1735–1744, 2019.
- [42] Hang Zhao, Chuang Gan, Andrew Rouditchenko, Carl Vondrick, Josh McDermott, and Antonio Torralba. The sound of pixels. In *Proceedings of the European conference on computer vision (ECCV)*, pages 570–586, 2018.
- [43] Hang Zhou, Xudong Xu, Dahua Lin, Xiaogang Wang, and Ziwei Liu. Sep-stereo: Visually guided stereophonic audio generation by associating source separation. In *European Conference on Computer Vision*, pages 52–69. Springer, 2020.